ACS OMEGA

http://pubs.acs.org/journal/acsodf

Article

Highly Efficient Organic Dyes Capture Using Thiol-Functionalized Porous Organic Polymer

Yan He,* Xiaolei Fu, Bo Li,* Haitao Zhao, Dingzhong Yuan, and Bing Na

Cite This: *ACS Omega* 2022, 7, 17941−17947

Read Online

ACCESS | Metrics & More | Article Recommendations | Supporting Information

ABSTRACT: It is of great significance to develop new materials for efficient capture cationic dyes methylene blue (MB) and malachite green (MG). In this work, a novel triptycene-based porous organic polymer with abundant thiol groups (TPP-SH) was prepared successfully by postmodification with a high surface area and robust triptycene-based porous organic polymer (TPP). The obtained TPP-SH exhibited a high surface area, good porosity, and good thermal stability. In addition, TPP-SH was highly effective at capturing MB and MG from aqueous solution because of the abundant thiols in its hierarchical structure. Under optimal adsorption conditions, the maximum adsorption capacities of MB and MG calculated by the Langmuir model at room temperature were 1146.3 and 689.6 mg g^{-1}, respectively. These values are higher than those of many reported materials. The MB and MG adsorption rates were 0.0154 and 6.69 × 10^{-4} mg g^{-1} min^{-1}, respectively. Furthermore, the polymer TPP-SH had a good recycling performance after adsorption−desorption at least five times. Therefore, the TPP-SH exhibited a high adsorption capacity, fast adsorption kinetics, and easy-recycling behavior, providing a new avenue for the preparation of green functionalized adsorbents with good performance for water decontamination.

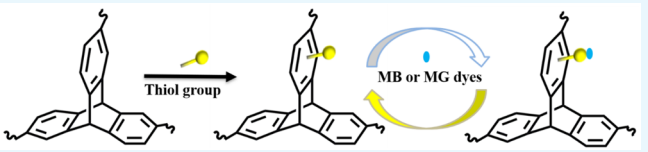

1. INTRODUCTION

With the development of industry, most organic dye pollutants from textiles, clothing, printing, and dyeing are discharged directly or indirectly into water. If they are not treated, they can cause harm to public health and damage to the ecosystem.[1] There are a large number of technologies for the removal of organic dye pollutants from wastewater, including adsorption, photocatalysis, biodegradation, membrane filtration, etc.[2−6] Among the various removal technologies, adsorption is considered to be a very efficient method to capture those ionic dyes because of its easy operation, low cost, and recyclability.[7,8] Many traditional porous materials, such as activated carbon,[9] lignin,[10] zeolitic imidazole frameworks (ZIFs),[11] and metal−organic frameworks (MOFs)[12] have been extensively reported. However, these materials suffer from low capacity, efficiency, and long times. To solve this series of problems, it is of great significance and technical challenge to design new adsorbents for efficient adsorption and removal of ionic dyes.

As an emerging material, porous organic polymers (POPs) not only have high specific surface area, rich pore structure, and diversified synthesis methods,[13,14] but also the surface functional groups of adsorbents can change the acidity, alkalinity, hydrophilicity, and hydrophobicity of adsorbents, and can bond with the groups of organic dyes in water.[15] It has potential application prospect in treating dye-containing wastewater.[16,17] By introducing functional groups into the porous structure, the adsorption performance of the material to specific substances can be improved, which can be used to design and construct highly efficient polymers.

The removal efficiency of organic dyes largely depends on the functional groups on the surface of the adsorbent.[18,19] Many kinds of amine group functionalized porous polymers have been designed and developed to capture carbon dioxide[20,21] and support metal catalyst.[22] Except for the amine group, thiol group can also be functionalized on the surface of the materials[23,24] due to thiol groups involve the bonding of 3s/3p hybrid orbital with larger sulfur to 1s orbital with smaller hydrogen.[25] There are also lone pair electrons on sulfur, which can form insoluble thiol groups salt with some heavy metal salts.[26] Similarly, sulfonic acid groups functionalized porous organic polymer also have good adsorption relationship with cationic organic dyes because of lone pair electrons on sulfur.[27] However, to the best of our knowledge, the application of thiol porous organic polymers in the removal of organic dyes has not been reported.

In this study, a new type of triptycene-based porous organic polymer (TPP) was prepared by using Suzuki coupling reaction[28] with three-dimensional bulk skeleton structure triptycene. After modification, the thiol groups were evenly distributed on the material skeleton, and a new type of thiol-group-functionalized triptycene-based porous organic polymer

Received: March 2, 2022
Accepted: May 6, 2022
Published: May 18, 2022

(TPP-SH) was prepared. Then, a series of adsorption experiments were carried out, including adsorption isotherms and kinetics, the effect of pH, and regeneration of adsorbent TPP-SH. The great adsorption kinetics, large adsorption capacity, good reusability, and excellent stability make TPP-SH an efficient and fast adsorbent for the removal of organic dyes from aqueous solutions.

2. EXPERIMENTAL SECTION

2.1. Reagents and Materials. All of the purchased chemicals were of at least reagent grade and were used without further purification. Triptycene (98.0%), concentrated nitric acid, hydrazine tetrahydrate, 1,5-cyclodiene, *N*,*N*-dimethylformamide (DNF) solution, paraformaldehyde, and sulfur sodium hydride were purchased from Sigma-Aldrich America. Methylene blue and malachite green were purchased from TCL America, and all other solvents were purchased from Aladdin Chemical China.

2.2. Synthesis of Thiol-Functionalized Porous Organic Polymer (TPP-SH). The thiol-functionalized porous organic polymer (TTP-SH) was afforded by functionalizing star triptycene-based microporous polymer-II (STP-II).[29] As shown in Scheme 1, the polymer STP-II (200 mg) was added to a solution of paraformaldehyde (1.0 g), acetic acid (6 mL), phosphoric acid (3 mL) and concentrated hydrochloric acid (20 mL). The mixture was then sealed and heated to 90 °C for 3 days. The collected solids were washed with water and methanol and then dried under vacuum to produce yellow TPP-1-CH2Cl solids. Subsequently, the obtained TPP-1-CH_2Cl was mixed with sodium hydrogen sulfide (NaHS, 1.2 g) in 100 mL of EtOH under a N_2 atmosphere and stirred at 75 °C for 3 days. The precipitate was collected, washed with water and methanol, and finally dried to obtain yellow powder TPP-SH.

Scheme 1. Synthesis Route of Thiol-Functionalized Porous Organic Polymer (TPP-SH)

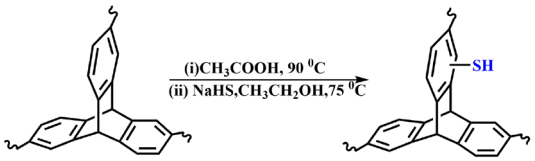

2.3. Instruments and Characterization. Transmission electron microscope (TEM) and high-resolution transmission electron microscope (HR-TEM) images were recorded on a JEM-2100 transmission electron microscope. The morphology of the samples was characterized using a Nova NanoS 450 field-emission scanning electron microscope (FE-SEM). The powder samples were treated in ethanol using ultrasound for 20 min and were then dropped and dried on carbon-coated copper grids. The powder X-ray diffraction (XRD) data were collected on a D/Max2550 VB/PC diffractometer (40 kV, 200 mA) using Cu K_α radiation. The N_2 adsorption desorption isotherms were measured at 77 K using a volumetric adsorption analyzer Micromeritics ASAP 2020. Before taking the adsorption measurements, the samples were degassed at 120 °C for 24 h. The specific surface areas were calculated using the Brunauer−Emmett−Teller (BET) method. The element analysis was performed on an elemental analyzer CHNS model (Thermo FLASH2000).

2.4. Adsorption Test. *Organic Dye Adsorption.* Two and a half milligrams of TPP-SH was added to 5 mL of MB and MG solution with an initial concentration of 1−1000 ppm under mechanical shaker conditions at a predetermined temperature (25, 35, 45 °C). After adsorption, the solution was filtered with 0.22 μm microporous PTFE membrane. The residual concentration of the dye was determined by UV−vis spectroscopy at the maximum wavelength. The adsorption capacity (q_e) and removal percentage of dyes (R %) were calculated by the following equations:

$$q_e = \frac{(C_0 - C_e)V}{m}$$

$$R\% = \frac{(C_o - C_e)}{C_o}100\%$$

C_0 (mg L^{-1}) represents the initial concentration of dyes. C_e (mg L^{-1}) and q_e (mg g^{-1}), respectively, represent the concentration and adsorption capacity of dyes at equilibrium.

Desorption Experiments and Reusability of TPP-SH. Fifty milligrams of porous polymer TPP-SH was added to the solution of MB and MG with an initial concentration of 50 ppm. After 24 h of adsorption, the adsorbent powder

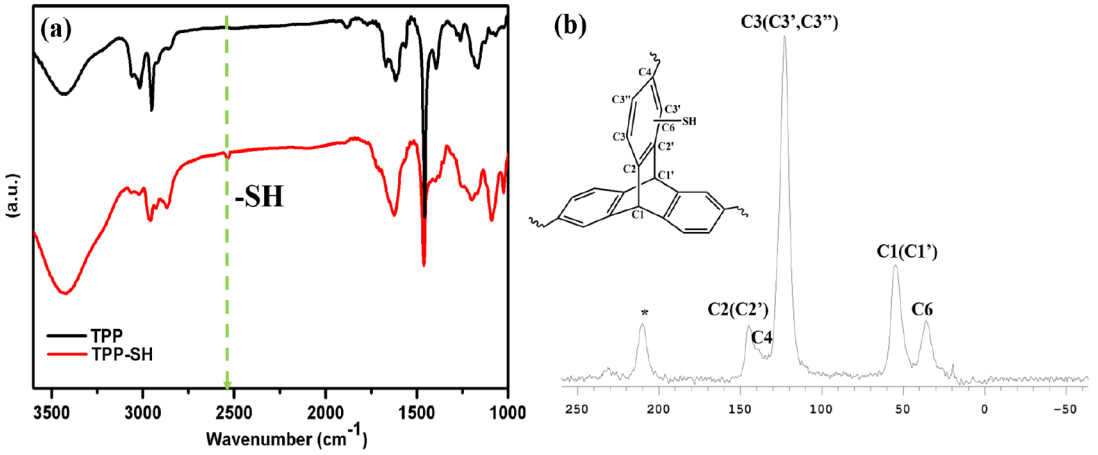

Figure 1. (a) FT-IR spectra of TPP-SH; (b) solid-state ^{13}C NMR spectra of TPP-SH.

https://doi.org/10.1021/acsomega.2c01250
ACS Omega 2022, 7, 17941−17947

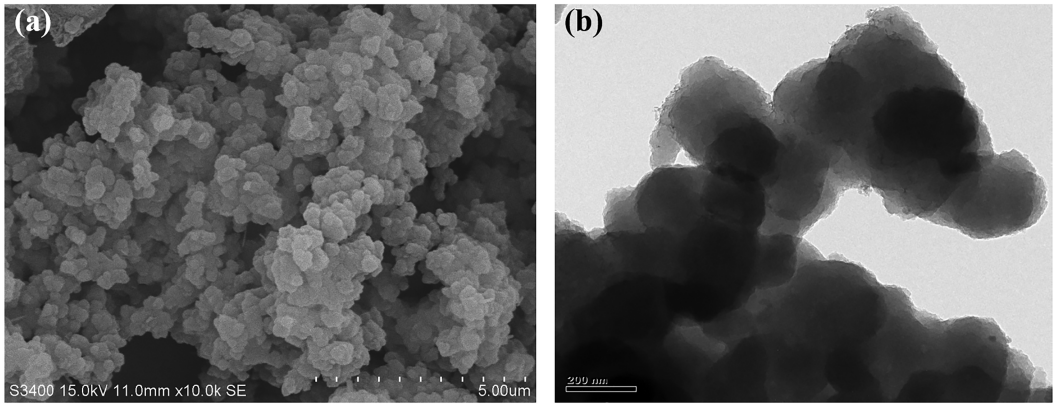

Figure 2. (a) SEM image of TPP-SH; (b) TEM image of TPP-SH.

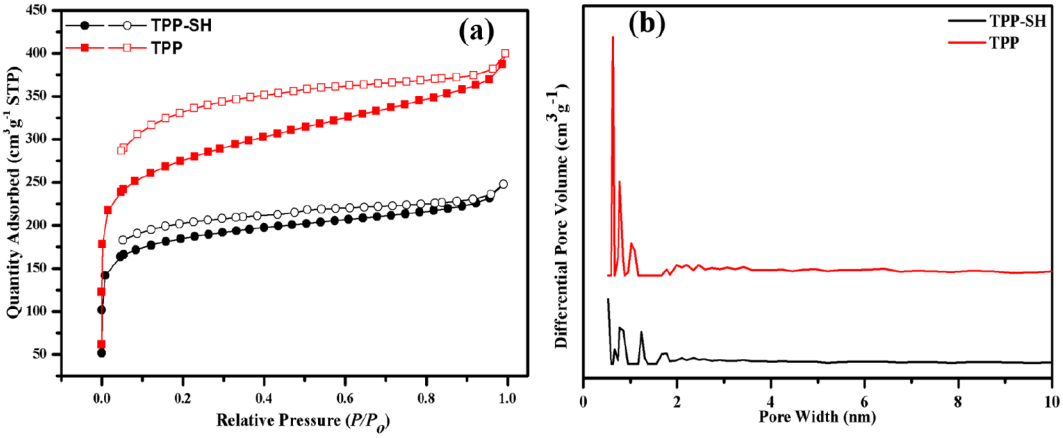

Figure 3. (a) N_2 adsorption−desorption isotherm of TPP-SH (black) and TPP (red). (b) Pore size distribution of TPP-SH (black) and TPP (red).

containing organic dye was washed with deionized water several times and then mixed and stirred in 100 mL 0.1 M HCl solution for 24 h to fully remove organic dye molecules. It was then washed with 100 mL of 0.1 M NaOH solution to remove the residual HCl. Finally, it was washed with ethanol and deionized water and dried in a vacuum for the next adsorption experiment.

3. RESULTS AND DISCUSSION

3.1. Characterization of TPP-SH. The structure of TPP-SH was characterized by Fourier transform infrared spectroscopy (FT-IR) and solid-state ^{13}C NMR. The FT-IR spectra (Figure 1a) of the TPP-SH show the characteristic band of S−H at 2577 cm^{-1}[30] compared with the pristine TPP. Furthermore, solid-state ^{13}C NMR confirmed the successful attachment of $-CH_2SH$ groups to the phenyl rings in TPP. As shown in Figure 1, the chemical shifts at 36.27 ppm can be assigned to the $-CH_2SH$ carbon C6. And the chemical shifts δ = 144.92, 141.81, 122.83, and 54.79 ppm can be assigned to the aromatic carbon C2(C2′), C4, C3(C3′,C3″), and the methylidyne bridge carbon C1(C1′), respectively. The content of S in the TPP-SH was 24.1% (Figure S1), which played a key role in the adsorption of dyes.

The morphology and crystalline nature of TPP-SH were investigated by SEM, TEM, and XRD. As show in Figure 2a, TPP-SH is composed of a spheroidal morphology with particle size ∼100 nm, where is the same with the pristine TPP (Figure S2). TEM image (Figure 2b) further gives the support to the SEM results and HR-TEM images (Figure S3) show that TPP-SH possess amorphous microporosity. In addition, without any characteristic peaks in all XRD patterns (Figure S4a), it strongly confirms the amorphous nature of microporous TPP-SH. Thermal gravimetric analysis (TGA) shows that TPP-SH is stable up to 200 °C (Figure S4b). The initial small weight loss below 100 °C would be mainly caused by the release of entrapped solvent or some small gaseous molecules in the micropores. The obtained TPP-SH is insoluble in dilute solutions of NaOH and HCl, as well as common organic solvents, such as dichloromethane, acetone, methanol, THF, and DMF, indicating good chemical stability of the TPP-SH adsorbent polymer.

The surface area and porosity of TPP-SH was measured at 77 K using N_2 adsorption−desorption isotherms. As shown in Figure 3a, under low pressure ($p/p_0 < 0.1$), the rapid increase of N_2 uptake indicates the existence of a large number of micropores. The presence of a hysteresis loop in the pressure region of p/p_0 = 0.2−0.8 suggests a partial mesoporous character. The hysteresis loop up to a relative pressure above 0.8 suggests the existence of macropores and interparticular voids. The porous properties of TPP and TPP-SH are summarized in (Table S1). The grafting of thiol groups leads to a decrease in the Brunauer−Emmett−Teller (BET) surface area from 919.7 for TPP to 607.1 $m^2\ g^{-1}$ for TPP-SH. The pore size distribution (PSD) calculated using the nonlocal density functional theory (NL-DFT) methods (Figure 3b) also confirmed the presence of primary micropore and a spot of meso- and macropore, which may be a resulted of the intrinsic

https://doi.org/10.1021/acsomega.2c01250
ACS Omega 2022, 7, 17941−17947

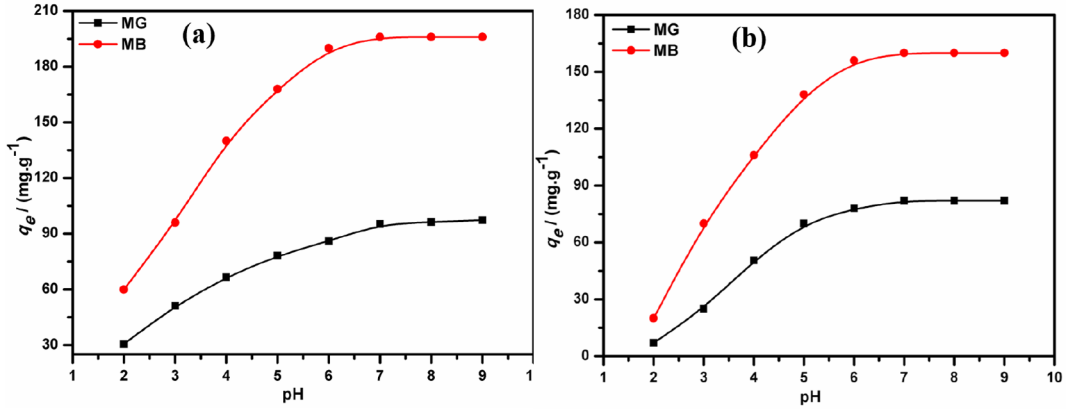

Figure 4. (a) pH effect on MB and MG adsorption performance on TPP-SH; (b) pH effect on MB and MG adsorption performance on TPP (MB concentration, 100 ppm; and MG concentration, 50 ppm).

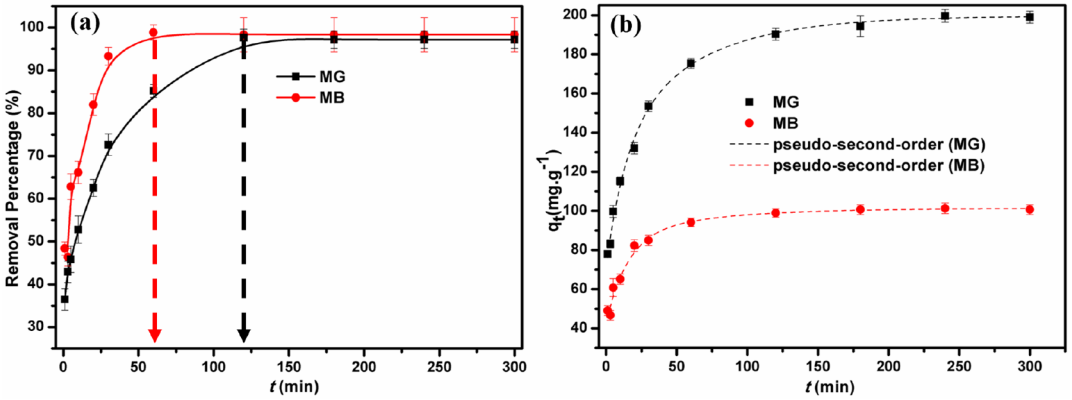

Figure 5. (a) Polymer TPP-SH adsorption dyes at different times; (b) plots of the pseudo-second-order kinetics for the adsorption of dyes (MB concentration, 50 ppm; and MG concentration, 100 ppm).

porosity and expanded networks of triptycenes. It is worth noting that the PSD hardly changed after the grafting of thiol groups.

3.2. pH Effect on the Adsorption of MB and MG on TPP-SH. The pH of the solution environment can affect the charge and stability of the adsorbents, which directly affects the strength of the interaction force between the cationic dyes and adsorbents. At the pHzpv (zero potential value), the surface has zero net charge (Figure S5). When the pH value (pH < pHzpv) is low, the adsorbents TPP-SH and TPP are protonated, and there is electrostatic repulsion between adsorbents and cationic dyes MB and MG, which may be an important factor leading to small adsorption capacity. As the pH value (pH > pHzpv) increases, the electrostatic repulsion between the adsorbent and MB and MG decreases, so the adsorption capacity increases. From the Figure 4, when the pH reaches a certain value (pH 7), the adsorption capacity reaches a plateau. Meanwhile, from Figure 4b, it can be seen that the adsorption capacity of MB and MG on TPP-SH is much higher than that of TPP (Table S2) because of the electrostatic interaction between the group −SH and dyes. Hence, we choose the above pH (pH 7) as experimental conditions when we study adsorption kinetics, adsorption isotherms, and thermodynamics.

3.3. Adsorption Kinetics of MB and MG on TPP-SH. To evaluate the effectiveness of TPP-SH for removing MG and MB from water, we investigated the effect of time on the adsorption of MB and MG by TPP-SH. As shown in Figure 5a, more than 99% of MB could be removed from water within 60 min. It is worth mentioning that the TPP-SH can capture MB two times faster than it can capture MG ions. Considering the great reliability to represent the kinetics for the adsorption of dyes from aqueous solutions onto TPP-SH, the experimental data were fitted with the pseudo-second-order kinetic model. As shown in Figure 5b and Table 1, an extremely high correlation coefficient (R^2 > 0.999) can be obtained from a pseudo-second-order dynamics model. This indicates that the adsorption rate of TPP-SH adsorbent to organic dyes depends on the availability of adsorption sites.

Table 1. Pseudo-Second-Order Kinetic Parameters for the Adsorption of MB and MG

dyes	$q_{e\ (expt)}$ (mg g^{-1})	$q_{e\ (calcd)}$ (mg g^{-1})	k_2 (g mg^{-1} min^{-1})	R^2
MG	201.34	203.25	6.69×10^{-4}	0.999
MB	99.96	100.02	0.0154	0.999

3.4. Adsorption Isotherms of MB and MG on TPP-SH. The adsorption isotherms at three different temperatures (25−45 °C) were studied. As shown in the Figure 6a, b, with the increase in the initial concentration of MB and MG, the adsorption capacity of MB and MG increased, indicating that MB and MG adsorbed well on high concentration. The experiment adsorption isotherms were fitted well with the Langmuir model. This indicates that the active sites have the same attraction to the adsorbates, which leads to a uniform

https://doi.org/10.1021/acsomega.2c01250
ACS Omega 2022, 7, 17941−17947

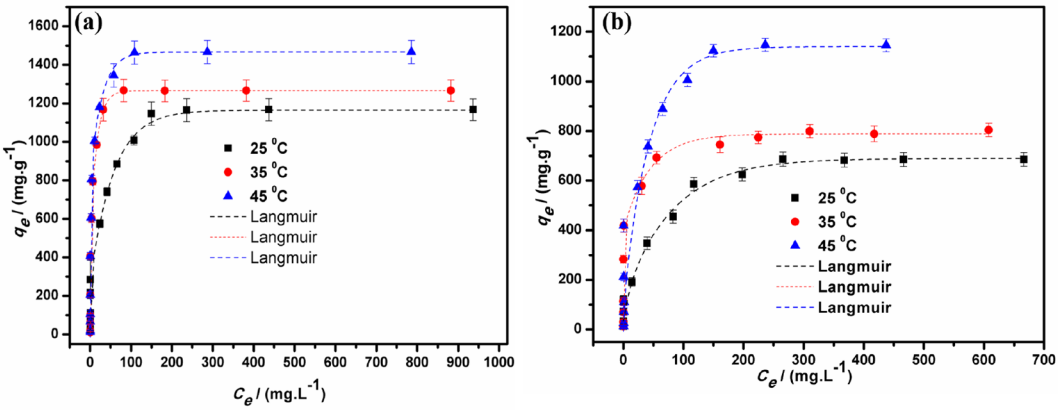

Figure 6. (a) Adsorption isotherm of TPP-SH on MB; (b) adsorption isotherm of TPP-SH on MG.

monolayer adsorption of dyes on the surface of TPP-SH. Furthermore, the maximum adsorption capacity calculated by the Langmuir model at room temperature is 1146.3 and 689.6 mg g^{-1}, respectively, because the negative functional group (−SH) can easily bind to cationic dyes through electrostatic interaction. The maximum adsorption capacity of MG increased from 1146.3 to 1434.2 mg g^{-1} and that of MB increased from 689.6 to 1166.8 mg g^{-1} in the temperature range from 25 to 45 °C. This indicates that the adsorption of TPP-SH on MB and MG has an endothermic effect at high temperature.[31,32]

From Table 2, the adsorption capacity of the TPP-SH adsorbent for MB and MG both higher than that of reported adsorbent polymers.[33−40] The excellent adsorption property of the novel polymer TPP-SH could be attributed to its large specific surface area, rich porosity, and even functional groups (−SH). Therefore, the polymer TPP-SH may be the most promising adsorbent as an efficient alterative for dye removal.

Table 2. Comparison of the Maximum Equilibrium Adsorption Capacity of the Dyes on Different Adsorbents at Room Temperature

adsorbents	BET (m^2 g^{-1})	q_{max} of dyes (mg g^{-1}) MB	MG	refs
MgO/graphene oxide composite	172.7	171.90	1275	33
peanut-shell-based activated carbon	170.4	-	306.06	34
monolithic activated carbon	566.49	299.52	-	35
ZIF-67	1445	5857.9	-	36
MCS	339	-	326.93	37
DT-POP	193	348.43	-	38
tannin-based magnetic POPs	110.7	1832	-	39
melamine-formaldehyde-tartaric acid resin	23.4	60.6	-	40
TPP-SH	607.11	1146.3	689.6	This work

3.5. Adsorption Thermodynamics of MB and MG on TPP-SH. Adsorption isotherms have been used to study the TPP-SH on different dyes at different temperatures. As shown in Table 3 and Figure S6, $\Delta H > 0$, $\Delta S > 0$, and $\Delta G < 0$, indicating that TPP-SH adsorption of MG/MB is a spontaneous endothermic and entropy increase reaction process. It is consistent with the results of adsorption isotherm experiments at different temperatures.

Table 3. Thermodynamic Parameters of MB and MG on TPP-SH

	ΔH (KJ mol^{-1})	ΔS (J mol^{-1})	ΔG(KJ mol^{-1}) at 25 °C	at 35 °C	at 45 °C
MG	66.32	250.66	−8.34	−10.96	−13.35
MB	83.33	298.46	−5.55	−8.92	−11.15

3.6. Desorption and Regeneration of TPP-SH. The pH studies and adsorption isotherms suggested that TPP-SH is an efficient MB and MG adsorbent because of its great porosity, large surface area, and thiol-functionalized group. So, in the study of the desorption process of TPP-SH on dyes, it was found that the MB and MG can be desorbed from TPP-SH by rinsing with hydrochloric acid. The desorption efficiency is up to 95%. To demonstrate the reusability of the TPP-SH, we repeated the adsorption−desorption cycle five times. As Figure 7 shows, During the adsorption−desorption cycle, the adsorption capacity of TPP-SH does not change significantly. The results show that the TPP-SH adsorbent is suitable for the efficient removal of dyes from an aqueous solution.

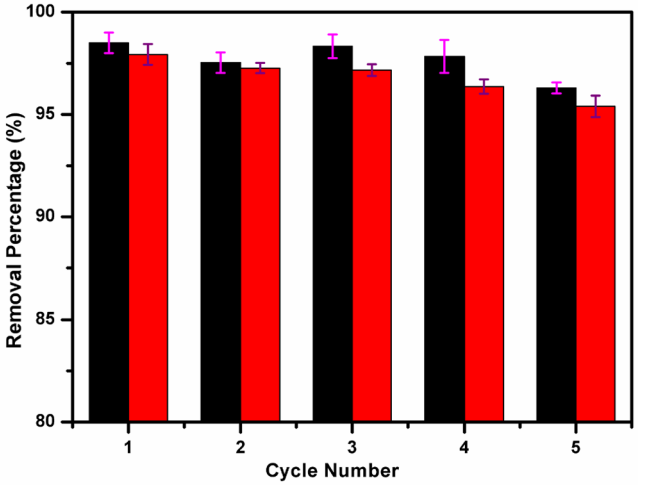

Figure 7. TPP-SH reusability of MG (black) and MB (red).

https://doi.org/10.1021/acsomega.2c01250
ACS Omega 2022, 7, 17941−17947

4. CONCLUSIONS

Novel triptycene-based porous organic polymers with abundant thiol groups (TPP-SH) were synthesized successfully by functionalizing a high-surface-area and robust triptycene-based porous organic polymer (TPP). The TPP-SH was highly effective in capturing MB and MG from aqueous solution. The adsorption behaviors of MB and MG on TPP-SH are in accordance with pseudo-second-order kinetics and fit the Langmuir model. The maximum adsorption capacities of MB and MG at room temperature were 1146.3 and 689.6 mg g^{-1}, respectively. Furthermore, the used TPP-SH could be effectively recycled at least five times and there is no obvious loss in adsorption capacity. Therefore, the TPP-SH has wide application prospects in the field of water purification and water treatment.

■ ASSOCIATED CONTENT

Supporting Information

The Supporting Information is available free of charge at https://pubs.acs.org/doi/10.1021/acsomega.2c01250.

Detailed adsorption experiment, figure of TPP-SH element analysis; SEM image of TPP; HR-TEM, XRD, and TG of TPP-SH; zeta potential of TPP-SH and TPP; table of the porous properties of TPP and TPP-SH (PDF)

■ AUTHOR INFORMATION

Corresponding Authors

Yan He − *Jiangxi Province Key Laboratory of Polymer Micro/Nano Manufacturing and Devices, School of Chemistry, Biology and Materials Science, East China University of Technology, Nanchang 330013, China;* orcid.org/0000-0002-4956-0733; Email: yanhe@ecit.edu.cn, yanheecust@163.com

Bo Li − *College of Engineering, Jiangxi Agricultural University, Nanchang 330045, China*; Email: bolee0086@sina.com

Authors

Xiaolei Fu − *Jiangxi Province Key Laboratory of Polymer Micro/Nano Manufacturing and Devices, School of Chemistry, Biology and Materials Science, East China University of Technology, Nanchang 330013, China*

Haitao Zhao − *Jiangxi Province Key Laboratory of Polymer Micro/Nano Manufacturing and Devices, School of Chemistry, Biology and Materials Science, East China University of Technology, Nanchang 330013, China*

Dingzhong Yuan − *Jiangxi Province Key Laboratory of Polymer Micro/Nano Manufacturing and Devices, School of Chemistry, Biology and Materials Science, East China University of Technology, Nanchang 330013, China;* orcid.org/0000-0003-2583-4071

Bing Na − *Jiangxi Province Key Laboratory of Polymer Micro/Nano Manufacturing and Devices, School of Chemistry, Biology and Materials Science, East China University of Technology, Nanchang 330013, China*

Complete contact information is available at: https://pubs.acs.org/10.1021/acsomega.2c01250

Notes

The authors declare no competing financial interest.

■ ACKNOWLEDGMENTS

Financial support for this work was provided by the National Science Foundation of China (21908022), the Jiangxi Provincial Natural Science Foundation (20202BAB213009), Jiangxi Provincial Key Innovation Project (202110405013), and the Scientific and Technical Project of the Educational Department in Jiangxi Province (GJJ18040303).

■ REFERENCES

(1) Karim, M. E.; Dhar, K.; Hossain, M. T. Decolorization of Textile Reactive Dyes by Bacterial Monoculture and Consortium Screened from Textile Dyeing Effluent. *J. Genet Eng. Biotechnol.* **2018**, *16* (2), 375−380.

(2) Maletić, M.; Vukčević, M.; Kalijadis, A.; Janković-Častvan, I.; Dapčević, A.; Laušević, Z.; Laušević, M. Hydrothermal synthesis of TiO_2 /carbon composites and their application for removal of organic pollutants. *Arab. J. Chem.* **2019**, *12* (8), 4388−4397.

(3) Verma, K. A.; Dash, R. R.; Bhunia, P. A review on chemical coagulation/flocculation technologies for removal of colour from textile wastewaters. *J. Environ. Manag.* **2012**, *93* (1), 154−168.

(4) Thangaraj, S.; Bankole, P. O.; Sadasivam, S. K. Microbial degradation of azo dyes by textile effluent adapted, Enterobacter hormaechei under microaerophilic condition. *Microbiol. Res.* **2021**, *250*, 126805.

(5) Yuan, D. Z.; Zhang, S.; Tan, J. L.; Dai, Y. H.; Wang, Y.; He, Y.; Liu, Y.; Zhao, X. H.; Zhang, M. M.; Zhang, Q. H. Highly efficacious entrapment of Th (IV) and U (VI) from rare earth elements in concentrated nitric acid solution using a phosphonic acid functionalized porous organic polymer adsorbent. *Sep. Purif. Technol.* **2020**, *237* (4), 116379.

(6) Mascarenhas, B. C.; Tavares, F. A.; Paris, E. C. Functionalized faujasite zeolite immobilized on poly(lactic acid) composite fibers to remove dyes from aqueous media. *J. Appl. Polym. Sci.* **2020**, *137*, 48561−48573.

(7) He, Y.; Bao, W. L.; Hua, Y. C.; Guo, Z. L.; Fu, X. L.; Na, B.; Yuan, D. Z.; Peng, C. J.; Liu, H. L. Efficient adsorption of methyl orange and methyl blue dyes by a novel triptycene-based hypercrosslinked porous polymer. *RSC Adv.* **2022**, *12*, 5587−5594.

(8) Yuan, D. Z.; Zhang, S.; Xiang, Z. H.; Liu, Y.; Wang, Y.; Zhou, X. Y.; He, Y.; Huang, W. J.; Zhang, Q. H. Highly Efficient Removal of Uranium from Aqueous Solution Using a Magnetic Adsorbent Bearing Phosphine Oxide Ligand: A Combined Experimental and Density Functional Theory Study. *ACS Sustain. Chem. Eng.* **2018**, *6* (8), 9619−9627.

(9) Kueasook, R.; Rattanachueskul, N.; Chanlek, N.; Dechtrirat, D.; Watcharin, W.; Amornpitoksuk, P.; Chuenchom, L. Green and facile synthesis of hierarchically porous carbon monoliths via surface self-assembly on sugarcane bagasse scaffold: Influence of mesoporosity on efficiency of dye adsorption. *Microporous Mesoporous Mater.* **2020**, *296*, 110005.

(10) Gonzalez-Lopez, M. E.; Robledo-Ortiz, J. R.; Rodrigue, D.; Perez-Fonseca, A. A. Highly porous lignin composites for dye removal in batch and continuous-flow systems. *Mater. Lett.* **2020**, *263*, 127289.

(11) Wu, X.; Xiong, J.; Liu, S.; Cheng, J.-H.; Zong, M.-H.; Lou, W.-Y. Investigation of hierarchically porous zeolitic imidazolate frameworks for highly efficient dye removal. *J. Hazard. Mater.* **2021**, *417* (417), 126011−126020.

(12) Hasanzadeh, M.; Simchi, A.; Far, H. S. Kinetics and adsorptive study of organic dye removal using water-stable nanoscale metal organic frameworks. *Mater. Chem. Phys.* **2019**, *233* (233), 267−275.

(13) Du, X. H.; Jiang, Z. Y.; Liu, Z. P.; Xu, C. BODIPY-linked conjugated porous polymers for dye wastewater treatment. *Microporous Mesoporous Mater.* **2022**, *332* (5), 111711.

(14) Gu, J. L.; Pi, W. Y.; Xie, W. F.; Gu, J. W.; Wang, Y. J.; Xiao, L.; Li, Y. J.; Li, J. F. Improved antibody adsorption performance of phenyl-based mixed-mode adsorbents by adjusting the functional group of ligand. *Biochem. Eng. J.* **2021**, *176* (12), 108092.

(15) He, Y.; Li, H.; Zhou, L.; Xu, T.; Peng, C. J.; Liu, H. L. Removal of Methyl Orange from Aqueous Solutions by a Novel Hyper-Cross-Linked Aromatic Triazine Porous Polymer. *Acta Phys.-Chim. Sin.* **2019**, *35* (3), 299−306.
(16) Cao, Y. P.; Liu, W.; Qian, J.; Cao, T.; Wang, J. M.; Qin, W. W. Porous Organic Polymers Containing a Sulfur Skeleton for Visible Light Degradation of Organic Dyes. *Chem.—Asian J.* **2019**, *14* (16), 2883−2888.
(17) Zhang, S. F.; Yang, M. X.; Qian, L. W.; Hou, C.; Tang, R. H.; Yang, J. F.; Wang, X. C. Design and preparation of a cellulose-based adsorbent modified by imidazolium ionic liquid functional groups and their studies on anionic dye adsorption. *Cellulose.* **2018**, *25* (6), 3557−3569.
(18) Li, Y. J.; Wang, H. J.; Zhao, W. F.; Wang, X. Q.; Shi, Y. D.; Fan, H. J.; Sun, H.; Tan, H. Facile synthesis of a triptycene-based porous organic polymer with a high efficiency and recyclable adsorption for organic dyes. *J. Appl. Polym. Sci.* **2019**, *136* (39), 47987.
(19) Farha, O. K.; Spokoyny, A. M.; Hauser, B. G.; Bae, Y. S.; Brown, S. E.; Snurr, R. Q.; Mirkin, C. A.; Hupp, J. T. Synthesis, properties, and gas separation studies of a robust diimide-based microporous organic polymer. *Chem. Mater.* **2009**, *21* (14), 3033−3035.
(20) Jovellana, J.; Pajarito, B. Carbon Dioxide Adsorbent Preparation by Coating Amine-Functionalized Pectin onto Zeolites. *Key Eng. Mater.* **2019**, *801*, 179−184.
(21) Wang, Y.; Du, T.; Song, Y.; Che, S.; Fang, X.; Zhou, L. Amine-functionalized mesoporous ZSM-5 zeolite adsorbents for carbon dioxide capture. *Solid State Sci.* **2017**, *73* (73), 27−35.
(22) Wang, X.; Han, X. Y.; Ren, F.; Xu, R. W.; Bai, Y. X. Porous Organic Polymers-Supported Metallocene Catalysts for Ethylene/1-Hexene Copolymerization. *Catalysts.* **2018**, *8* (4), 146.
(23) Zhang, Y.; Hong, X.; Cao, X. M.; Huang, X. Q.; Hu, B.; Ding, S. Y.; Lin, H. Functional Porous Organic Polymers with Conjugated Triaryl Triazine as the Core for Superfast Adsorption Removal of Organic Dyes. *ACS Appl. Mater. Interfaces.* **2021**, *13* (5), 6359−6366.
(24) Barczak, M.; Dobrowolski, R.; Borowski, P.; Giannakoudakis, D. A. Pyridine-, thiol-and amine-functionalized mesoporous silicas for adsorptive removal of pharmaceuticals. *Microporous Mesoporous Mater.* **2020**, *299* (299), 110132−110136.
(25) Asim, M. H.; Ijaz, M.; Mahmood, A.; Knoll, P.; Jalil, A.; Arshad, S.; Bernkop-Schnurch, A. Thiolated cyclodextrins: Mucoadhesive and permeation enhancing excipients for ocular drug delivery. *Int. J. Pharm.* **2021**, *599*, 120451.
(26) Liu, H. X.; Xie, X. J. Thiol-methyl-modified magnetic microspheres for effective cadmium (II) removal from polluted water. *Environ. Sci. Pollut. Res. Int.* **2021**, *28* (31), 42750−42762.
(27) Li, Y.; Wang, H.; Zhao, W.; Wang, X.; Shi, Y.; Fan, H.; Sun, H.; Tan, L.; et al. Facile synthesis of a triptycene-based porous organic polymer with a high efficiency and recyclable adsorption for organic dyes. *J. Appl. Polym. Sci.* **2019**, *136* (39), 47987.
(28) Esteban, N.; Ferrer, M. L.; Ania, C. O.; de la Campa, J. G.; Lozano, A. E.; Alvarez, C.; Miguel, J. A. Porous Organic Polymers Containing Active Metal Centers for Suzuki-Miyaura Heterocoupling Reactions. *ACS Appl. Mater. Interfaces* **2020**, *12* (51), 56974−56986.
(29) Zhang, C.; Liu, Y.; Li, B. Y.; Tan, B.; Chen, C. F.; Xu, H. B.; Yang, X. L. Triptycene-Based Microporous Polymers: Synthesis and Their Gas Storage Properties. *ACS Macro Lett.* **2012**, *1* (1), 190−193.
(30) Li, B. Y.; Zhang, Y. M.; Ma, D. X.; Shi, Z.; Ma, S. Q. Mercury nano-trap for effective and efficient removal of mercury(II) from aqueous solution. *Nat. Commun.* **2014**, *5*, 5537.
(31) Kenyo, C.; Kajtar, D. A.; Renner, K.; Krohnke, C.; Pukanszky, B. Functional packaging materials: factors affecting the capacity and rate of water adsorption in desiccant composites. *J. Polym. Res.* **2013**, *20*, 2−8.
(32) Lombardo, S.; Thielemans, W. Thermodynamics of adsorption on nanocellulose surfaces. *Cellulose* **2019**, *26*, 249−279.
(33) Guo, T.; Bulin, C. K. Facile fabrication of MgO/graphene oxide composite as an efficient adsorbent for rapid removal of aqueous organic dyes: Performance evaluation and mechanistic investigation. *J. Phys. Chem. Solids.* **2021**, *158*, 110251.
(34) Ahmad, M. A.; Yusop, M.; Zakaria, R.; Karim, J.; Abdullah, N. S. Adsorption of methylene blue from aqueous solution by peanut shell based activated carbon. *Mater. Today: Proc.* **2021**, *47*, 1246−1251.
(35) Hilbrandt, I.; Ruhl, A. S.; Jekel, M. Testing monolithic activated carbon adsorbers for in-line removal of organic micropollutants. *Water Sci. Technol.* **2016**, *16* (6), 1693−1699.
(36) Liu, Y. F.; Lin, D. Y.; Yang, W. T.; An, X. Y.; Sun, A. H.; Fan, X. L.; Pan, Q. H. In situ modification of ZIF-67 with multi-sulfonated dyes for great enhanced methylene blue adsorption via synergistic effect. *Microporous Mesoporous Mater.* **2020**, *303*, 110304.
(37) Li, H. J.; Miao, Q. S.; Chen, Y. L.; Yin, M. Y.; Qi, H.; Yang, M. C.; Deng, Q. L.; Wang, S. Modified carbon spheres as universal materials for adsorption of cationic harmful substances (paraquat and dyes) in water. *Microporous Mesoporous Mater.* **2020**, *297*, 110040.
(38) Shen, Y.; Ni, W. X.; Li, B. Porous Organic Polymer Synthesized by Green Diazo-Coupling Reaction for Adsorptive Removal of Methylene Blue. *ACS Omega.* **2021**, *6* (4), 3202−3208.
(39) Murugesan, A.; Divakaran, M.; Raveendran, P.; Nitin Nikamanth, A. B.; Thelly, K. J. An Eco-friendly Porous Poly(imide-ether)s for the Efficient Removal of Methylene Blue: Adsorption Kinetics, Isotherm, Thermodynamics and Reuse Performances. *J. Polym. Environ.* **2019**, *27*, 1007−1024.
(40) Huang, L.; Shuai, Q.; Hu, S. Tannin-based magnetic porous organic polymers as robust scavengers for methylene blue and leadions. *J. Clean. Prod.* **2019**, *215*, 280−289.

https://doi.org/10.1021/acsomega.2c01250
ACS Omega 2022, 7, 17941−17947